Estimating Diffusion Parameters from Polarized Spherical-Gradient Illumination

Yufeng Zhu and Pradeep Garigipati ▪ *University of Southern California Institute for Creative Technologies*

Pieter Peers ▪ *The College of William & Mary*

Paul Debevec and Abhijeet Ghosh ▪ *University of Southern California Institute for Creative Technologies*

The proposed method acquires subsurface-scattering parameters of heterogeneous translucent materials. It directly obtains dense per-surface-point scattering parameters from observations under cross-polarized spherical-gradient illumination of curved surfaces. This method does not require explicit fitting of observed scattering profiles. A variety of heterogeneous translucent objects illustrate its validity.

Accurately modeling and reproducing real-world materials' appearance are crucial for producing photorealistic imagery of digital scenes and subjects. The appearance of many common materials is due to subsurface light transport, which causes the characteristic "soft" appearance and the materials' unique coloring. To efficiently model isotropic subsurface light transport, Henrik Jensen and his colleagues introduced the dipole-diffusion approximation[1] (see the "Diffusion Models" and "Related Work" sidebars). The scattering parameters needed to drive this approximation are typically estimated by illuminating a homogeneous surface patch with either a collimated beam of light or, for spatially varying translucent materials, a dense set of structured light patterns. Most methods involve a trade-off between acquisition time and the scattering parameters' spatial density.

We have developed a method that estimates dense per-surface-point scattering parameters of a curved heterogeneous translucent material sample. Existing techniques employ spatial modulation of the incident illumination to estimate a translucent material's scattering parameters. Unlike other methods, ours relies on angular modulation of the incident illumination and surface curvature to infer the parameters. The acquisition cost is independent of the desired spatial resolution. In addition, our method obtains direct estimates of scattering parameters from only four cross-polarized measurements of the translucent sample under zeroth- and first-order spherical-gradient illumination (see Figure 1). Although our method is in theory limited to isotropic diffusive materials and isotropically curved surfaces, it has produced good results on a variety of heterogeneous translucent objects.

Motivation

Wan-Chun Ma and his colleagues proposed employing (four) polarized spherical-gradient lighting conditions to estimate photometric normals for both diffuse reflection (via cross-polarization) and specular reflection (via polarization differencing).[2] Ideally, both sets of normals should be identical. However, Ma and his colleagues observed that for translucent materials, the diffuse photometric normals were less sharp; this softness was wavelength dependent (see Figure 1e). They

Diffusion Models

In the main article we assume that the diffuse subsurface light transport of a translucent material can be accurately modeled by the dipole-diffusion approximation.[1] However, this model is strictly valid only for characterizing multiple scattering in a highly scattering homogeneous translucent medium in a semi-infinite planar material sample (Pat Hanrahan and Wolfgang Krueger proposed an analytical solution to single scattering[2]). Although the dipole-diffusion model is limited, it remains popular for both rendering and modeling owing to its relative simplicity.

Since that model's introduction, researchers have proposed more accurate or specialized models. Craig Donner and Jensen extended the model to multilayer translucent materials.[3] Donner and Jensen also proposed an extended source model to account for complex geometry, internal blockers, and so on.[4] However, these methods still rely on the diffusion approximation—namely, that the light distribution in a translucent medium becomes isotropic after a sufficient number of scattering events.

Donner and his colleagues developed a data-driven model to represent the full spatial and angular distribution of subsurface scattering.[5] However, this model is limited to planar, single-layer, semi-infinite translucent-material samples. Recently, Eugene D'Eon and Geoffrey Irving proposed the quantized diffusion model, which is based on a modified diffusion theory.[6] This model can accurately model translucent material that is highly absorbing or consists of thin layers.

References

1. H.W. Jensen et al., "A Practical Model for Subsurface Light Transport," *Proc. Siggraph*, ACM, 2001, pp. 511–518.
2. P. Hanrahan and W. Krueger, "Reflection from Layered Surfaces Due to Subsurface Scattering," *Proc. Siggraph*, ACM, 1993, pp. 165–174.
3. C. Donner and H.W. Jensen, "Light Diffusion in Multi-layered Translucent Materials," *ACM Trans. Graphics*, vol. 24, no. 3, 2005, pp. 1032–1039.
4. C. Donner and H.W. Jensen, "Rendering Translucent Materials Using Photon Diffusion," *Proc. 18th Eurographics Conf. Rendering Techniques*, Eurographics Assoc., 2007, pp. 243–251.
5. C. Donner et al., "An Empirical BSSRDF Model," *ACM Trans. Graphics*, vol. 28, no. 3, 2009, article 30.
6. E. D'Eon and G. Irving, "A Quantized-Diffusion Model for Rendering Translucent Materials," *ACM Trans. Graphics*, vol. 30, no. 4, 2011, article 56.

speculated that one source of the apparent difference was subsurface light transport.

Here, we formalize the connection between a translucent material's scattering properties and the reflectance observations under polarized spherical-gradient illumination. First, we establish an empirical connection to inform the formal derivations. We employ the cross-polarized reflectance observations where polarization-preserving scattering events (specular reflections and single scattering) have been canceled out. This leaves only the reflectance due to subsurface scattering.

Furthermore, as Abhijeet Ghosh and his colleagues noted,[3] the reflectance observed under cross-polarized constant lighting is related to the reduced albedo α', one of the three parameters required for the dipole-diffusion approximation of subsurface scattering.[1] As in prior research, we fix the index of refraction η to 1.4 (the index of refraction of skin, and a good median for many organic materials), leaving the diffusion constant D as the only free parameter.

For materials for which the diffusion approximation is valid, the *bidirectional surface scattering reflectance distribution function* (BSSRDF) reduces to a 4D function $R_d(x_o, x_i)$ between entrance points x_i and exitance points x_o over the object surface. We can then define the diffuse BSSRDF R_d as

$$R_d(r) = -D \frac{(\mathbf{n} \cdot \nabla\phi)(x_o)}{d\Phi_i(x_i)},$$

where $r = \|x_o - x_i\|$.[1]

Inspired by this equation, which relates R_d and D via a spatial gradient, we look at the ratio of the observations under constant spherical lighting to the observations under gradient illumination along the surface normal (that is, $\mathbf{n}$ points toward the brightest point on the angular gradient, $I_N(\omega) = \mathbf{n} \cdot \omega$, where ω is the direction) for a curved surface. First, we empirically observe that the ratio is approximately proportional to D and that the relation is roughly linear. Second, the slope is inversely proportional to the albedo and surface curvature.

This motivates us to consider a linear approximation of D for the dipole model as

$$D = (ratio - \min Ratio)\frac{slope}{\kappa}, \qquad (1)$$

where

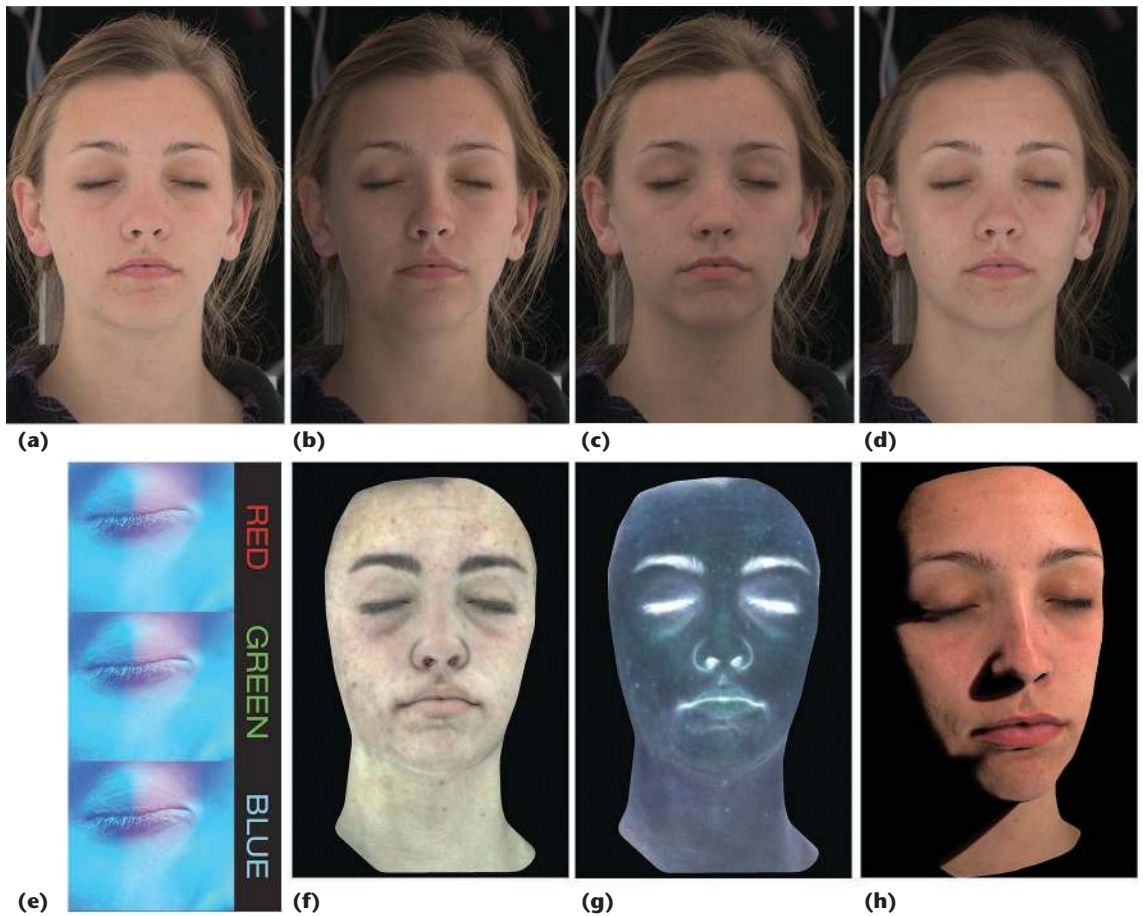- *ratio* is the observed reflectance under constant

Figure 1. Estimating diffusion parameters. Under cross-polarized zeroth-order and first-order spherical-gradient illumination conditions, we observe the (a) diffuse albedo and the (b) *x*, (c) *y*, and (d) *z* gradients. We use the (e) diffuse normals to determine the curvature. The observations enable us to obtain the per-surface-point diffusion parameters for (f) translucency and (g) absorption. The estimated scattering parameters can subsequently be used in (h) dipole-diffusion rendering.

spherical lighting divided by the observed reflectance under a linear spherical-gradient illumination (aligned along **n**),

- min*Ratio* = 1.184 is the ratio for a nontranslucent material, and
- *slope* is empirically determined as $(2(1 - R_d)^2 + 0.75)(0.8 + 2/(100\kappa))$, where R_d is the diffuse albedo and κ is the mean surface curvature.

The ratio assumes a linear spherical gradient with intensities ranging from 0 to 1 along the surface normal's direction.

Figure 2 shows simulated plots of this approximation versus the true diffusion constant for different spherical surfaces. The estimated scattering parameters' overall accuracy is very good for high-curvature surfaces (that is, a small radius), while degrading gracefully with decreasing curvature (that is, an increasing radius).

The Analytic Formulation

The linear approximation in Equation 1 shows

that the scattering and absorption coefficients, a spatial property, can be inferred from observations under angularly varying lighting. The linear approximation yields good estimates of scattering parameters for typical ranges of albedo, translucency, and curvature. However, it remains an empirical approximation with significant errors for very low albedo values and flat surfaces with low curvatures. So, we formally derived an analytic formulation relating *ratio* and *D* based on the dipole-diffusion theory.

In particular, we observe the material sample under these four lighting conditions: $I_X(\omega) = \omega_x$, $I_Y(\omega) = \omega_y$, $I_Z(\omega) = \omega_z$, and $I_1(\omega) = 1$, where ω_x, ω_y, and ω_z are the *x*, *y*, and *z* components of ω. We polarize the incident lighting according to the polarization pattern proposed by Ma and his colleagues,[2] which lets us use cross-polarization to eliminate polarization-preserving reflectance (that is, specular reflections and single scattering) toward the camera. So, we observe only diffuse reflectance, which we approximate at x_o in direction ω_o by

Related Work in Measuring Subsurface-Scattering Properties

Capturing and modeling the *bidirectional surface scattering reflectance distribution function* (BSSRDF)[1] of translucent materials is a challenge. Most techniques rely on the diffusion approximation, which reduces from eight to four the number of BSSRDF dimensions to sample.[2] Henrik Jensen and his colleagues introduced the dipole-diffusion model to describe homogeneous translucent materials, which relies on a only few parameters (absorption and scattering).[3] Jensen and his colleagues inferred these parameters from observations of a homogeneous planar translucent-material sample illuminated by a tightly focused beam of white light. However, no such compact model exists for heterogeneous subsurface-scattering materials, and acquisition is difficult.

Michael Goesele and his colleagues modeled the subsurface-scattering properties of heterogeneous translucent materials by directly using the subsurface responses observed from sequentially scanning the translucent object's surface with a laser.[4] Pieter Peers and his colleagues sped up the acquisition of heterogeneous subsurface scattering by projecting and shifting a dot pattern over the surface, effectively observing multiple subsurface-scattering profiles at once.[5] Xin Tong and his colleagues inferred scattering parameters by sweeping a laser strip over the sample.[6] All these methods rely on some form of spatial scanning to infer per-surface-point subsurface-scattering parameters. So, the acquisition cost is directly proportional to the desired spatial resolution. In contrast, the acquisition cost of our method (see the main article) is independent of the spatial resolution.

Another class of methods focuses on a particular subclass of materials such as human skin. Tim Weyrich and his colleagues observed that skin's BSSRDF varies slowly spatially.[7] They proposed capturing per-region subsurface-scattering properties using a specially designed probe. Similarly, Abhijeet Ghosh and his colleagues captured a per-region BSSRDF from observations of the subject illuminated by a single dot pattern.[8] Craig Donner and his colleagues inferred the per-surface-point concentration of chromophores in human skin from multispectral observations under constant illumination.[9] Although these methods' capture cost is small and independent of the spatial resolution, they are suited only for modeling skin's subsurface-scattering properties. In contrast, for a comparable acquisition cost, our method provides a per-surface-point estimate of the BSSRDF of arbitrary translucent materials.

References

1. F.E. Nicodemus et al., "Geometric Considerations and Nomenclature for Reflectance," monograph 160, US Nat'l Bureau of Standards, 1977.
2. J. Stam, "Multiple Scattering as a Diffusion Process," *Proc. Eurographics Rendering Workshop,* Eurographics Assoc., 1995, pp. 41–50.
3. H.W. Jensen et al., "A Practical Model for Subsurface Light Transport," *Proc. Siggraph,* ACM, 2001, pp. 511–518.
4. M. Goesele et al., "Disco: Acquisition of Translucent Objects," *ACM Trans. Graphics,* vol. 23, no. 3, 2004, pp. 835–844.
5. P. Peers et al., "A Compact Factored Representation of Heterogeneous Subsurface Scattering," *ACM Trans. Graphics,* vol. 25, no. 3, 2006, pp. 746–753.
6. X. Tong et al., "Modeling and Rendering of Quasi-homogeneous Materials," *ACM Trans. Graphics,* vol. 24, no. 3, 2005, pp. 1054–1061.
7. T. Weyrich et al., "Analysis of Human Faces Using a Measurement-Based Skin Reflectance Model," *ACM Trans. Graphics,* vol. 25, no. 3, 2006, pp. 1013–1024.
8. A. Ghosh et al., "Practical Modeling and Acquisition of Layered Facial Reflectance," *ACM Trans. Graphics,* vol. 27, no. 5, 2008, article 139.
9. C. Donner et al., "A Layered, Heterogeneous Reflectance Model for Acquiring and Rendering Human Skin," *ACM Trans. Graphics,* vol. 27, no. 5, 2008, article 140.

$$L(x_o, \omega_o) =$$
$$\frac{1}{\pi} \int_A \int_\Omega F_t(\eta, \mathbf{n}(x_o) \cdot \omega_o)$$
$$\times R_d(x_i, x_o) F_t(\eta, \mathbf{n}(x_i) \cdot \omega_i)$$
$$\times L_i(x_i, \omega_i)(\mathbf{n}(x_i) \cdot \omega_i) d\omega_i dx_i,$$

where $L_i(x_i, \omega_i)$ represents the incident lighting from ω_i at x_i.[1] F_t is the Fresnel transmittance term with the index of refraction η, which we assume is constant over the sample. $\mathbf{n}(x_i)$ is the surface normal at x_i, and R_d is the diffuse subsurface scattering between x_i and x_o.

We now consider the canonical cases in which L_i is the constant-lighting condition I_1 and the gradient aligned with the surface normal at x_o is $I_N(\omega) = \mathbf{n}(x_o) \cdot \omega$. Without loss of generality, we express variables in the normal's coordinate system (z points up, so $I_N(\omega) = \omega_z$):

$$L_{I_N}(x_o, \omega_o) =$$
$$\frac{F_t(\eta, \omega_{o_z})}{\pi}$$
$$\int_A R_d(x_i, x_o)$$
$$\int_\Omega F_t(\eta, \mathbf{n}(x_i) \cdot \omega_i)(\mathbf{n}(x_i) \cdot \omega_i) I_N(\omega_i) d\omega_i dx_i.$$

We observe that $F_t(\eta, \mathbf{n}(x_i) \cdot \omega_i)(\mathbf{n}(x_i) \cdot \omega_i)$ is a symmetric function around $\mathbf{n}(x_i)$. This allows us to follow a similar reasoning as Ma and his colleagues'
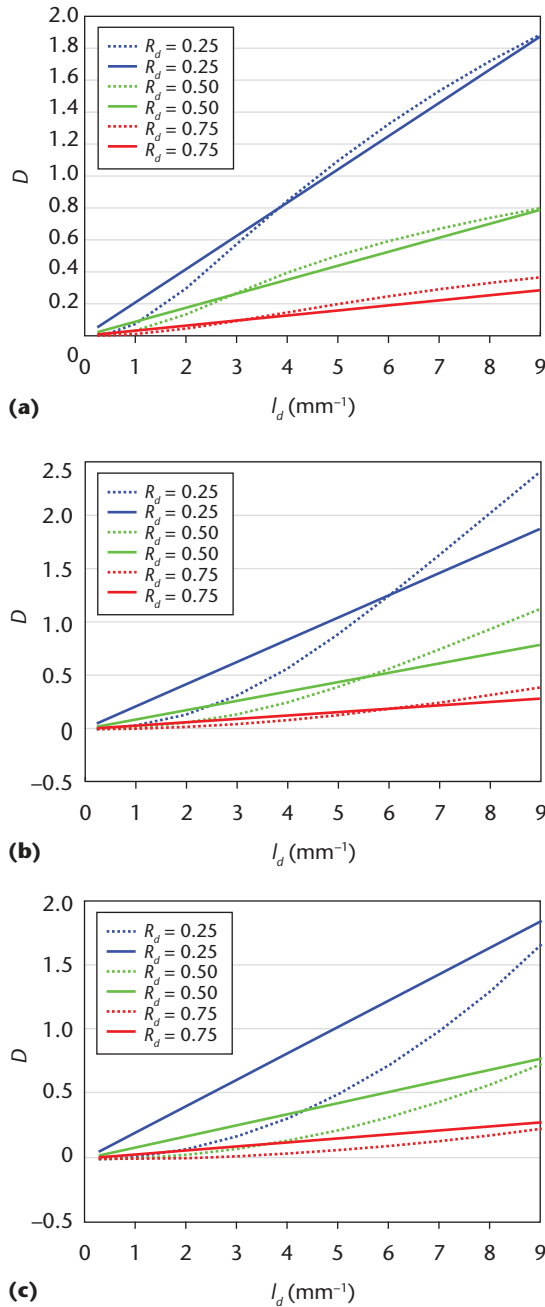
Figure 2. Simulated plots of the true diffusion constant (solid lines) versus the linear approximation (dashed lines), for radii of (a) 10, (b) 30, and (c) 100 mm. R_d is the diffuse albedo, D is the diffusion constant, and l_d is the translucency. We obtained the approximations from the ratio of the observed reflectance under constant spherical lighting to the observed reflectance under spherical-gradient (aligned along the surface normal) lighting for different albedos and spherical surfaces (with different curvatures $\kappa = 1/\text{radius}$).

derivation for diffuse reflectance.[2] Taking the inner product over $I_N(\omega_i)$ with $F_t(\eta, \mathbf{n}(x_i) \cdot \omega_i)(\mathbf{n}(x_i) \cdot \omega_i)$ yields the z component of $\mathbf{n}_z(x_i)$ times a constant $C_z(\eta)$ that depends only on the index of refraction and that is independent of the surface normal:

$$L_{I_N}(x_o, \omega_o) = \frac{F_t(\eta, \omega_{o_z}) C_z(\eta)}{\pi}$$
$$\int_A R_d(x_i, x_o) \mathbf{n}_z(x_i) dx_i.$$

Furthermore, we assume that the shape of the curved surface sample's local neighborhood is isotropic and can be expressed in terms of the mean spherical curvature κ: $\mathbf{n}_z(x_i) = \cos(\kappa r)$, where $r = \|x_i - x_o\|$.

Rewriting in terms of polar coordinates (r, θ) yields

$$L_{I_N}(x_o, \omega_o) = \frac{F_t(\eta, \omega_{o_z}) C_z(\eta)}{\pi}$$
$$\int_0^{2\pi} \int_0^\infty R_d(r) r \cos(\kappa r) dr\, d\theta$$
$$= 2 F_t(\eta, \omega_{o_z}) C_z(\eta)$$
$$\int_0^\infty R_d(r) r \cos(\kappa r) dr$$
$$= 2 F_t(\eta, \omega_{o_z}) C_z(\eta) R_c(x_o, \kappa), \qquad (2)$$

where

$$R_c(x_o, \kappa) = \int_0^\infty R_d(r) r \cos(\kappa r) dr.$$

Similarly, setting $L_i(\omega_i) = I_1(\omega_i)$ yields

$$L_{I_1}(x_o, \omega_o) = \frac{F_t(\eta, \omega_{o_z}) C_f(\eta)}{\pi}$$
$$\int_0^{2\pi} \int_0^\infty R_d(r) r \, dr\, d\theta$$
$$= 2 F_t(\eta, \omega_{o_z}) C_f(\eta)$$
$$\int_0^\infty R_d(r) r \, dr$$
$$= 2 F_t(\eta, \omega_{o_z}) C_f(\eta) R_c(x_o, 0), \qquad (3)$$

where $C_f(\eta)$ is the corresponding constant for $F_t(\eta, \mathbf{n}(x_i) \cdot \omega_i)(\mathbf{n}(x_i) \cdot \omega_i)$ under I_1, and $R_c(x_o, 0)$ (times 2π) is equivalent to the diffuse albedo R_d at x_o.[1]

Equations 2 and 3 both consist of one part that depends solely on the index of refraction and another part that depends on the scattering parameters (including the index of refraction) and curvature. Whereas $C_z(\eta)$ and $C_f(\eta)$ vary significantly with the index of refraction, their ratio $C_f(\eta)/C_z(\eta)$ is approximately constant for common indices of refraction (that is, monotonically decreasing from 1.5 for a 1.0 index of refraction to 1.454 for a 1.5 index of refraction). So, we can approximate the ratio of the observed reflectance under constant spherical lighting to the observed reflectance under normal aligned spherical-gradient lighting by

$$ratio(x_o) = \frac{L_{I_1}(x_o, \omega_o)}{L_{I_N}(x_o, \omega_o)}$$

$$\approx 1.456 \frac{R_c(x_o, 0)}{R_c(x_o, \kappa)}, \qquad (4)$$

where we opt for $C_f(\eta)/C_z(\eta) \approx 1.456$ (that is, the ratio for $\eta = 1.4$).

Next, we derive analytical expressions for $R_c(x_o, 0)$ and $R_c(x_o, \kappa)$ and show how to estimate the spatially varying $\alpha'(x_o)$ and $D(x_o)$ from $L_{I_1}(x_o, \omega_o)$ and $ratio(x_o)$, respectively. For compactness and clarity, we omit x_o.

To estimate α', we first note that

$$R_d = \frac{\pi L_{I_i}(\omega_o)}{F_t(\eta, \omega_{o_z}) C_f(\eta)}.$$

Jensen and his colleagues proposed the following analytical solution for R_d:

$$R_d = \frac{\alpha'}{2}\left[1 + e^{-\frac{4}{3}A\sqrt{3(1-\alpha')}}\right]e^{-\sqrt{3(1-\alpha')}}, \qquad (5)$$

where A is the internal reflection that depends on η.[1] We employ Newton's method for finding α' from R_d, and thus from the constant observations $L_{I_1}(\omega_o)$, assuming $\eta = 1.4$ and setting the initial starting point at $1 - \epsilon$.

To find an approximate analytical expression for $R_c(\kappa)$, we replace the cosine by a second-order Taylor expansion around zero (see the sidebar, "An Analytical Formulation for $R_c(\kappa)$"). Using the shorthand notations

$$g = \sqrt{3(1-\alpha')},$$

$$b = \frac{4}{3}A,$$

$$z = \left(1 + e^{-\frac{4}{3}A\sqrt{3(1-\alpha')}}\right),$$

we find that

$$R_c(\kappa) =$$

$$\frac{\alpha'}{4\pi}\left[\begin{bmatrix}1 - \frac{(3D\kappa)^2}{g}\end{bmatrix} + \left(1 - \frac{(3D\kappa)^2(1+b)}{g}\right)e^{-bg}\right]e^{-g}. \qquad (6)$$

Combining Equations 4, 5, and 6 yields

$$ratio \approx 1.456 \frac{z}{z - \frac{(3D\kappa)^2}{g}\left(z + be^{-bg}\right)},$$
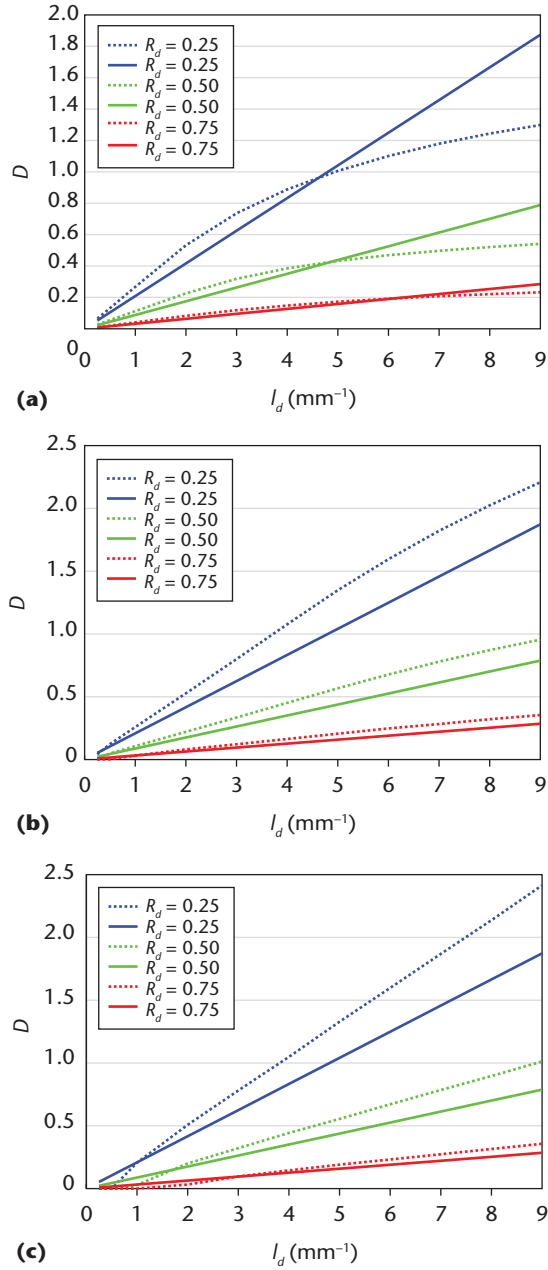
(a)

(b)

(c)

Figure 3. Simulated plots of the true diffusion constant (solid lines) versus the analytic formulation (dashed lines), for radii of (a) 10, (b) 30, and (c) 100 mm. We obtained the approximations from the ratio of the observed reflectance under constant spherical lighting to the observed reflectance under spherical-gradient (aligned along the surface normal) lighting for different albedos and spherical surfaces.

from which we can relate D to $ratio$:

$$D \approx \frac{1}{3\kappa}\sqrt{g\frac{z - 1.456\frac{z}{ratio}}{z + be^{-bg}}}. \qquad (7)$$

Figure 3 shows simulated plots of estimates obtained from Equation 7 versus the true diffusion

An Analytical Formulation for $R_c(\kappa)$

To derive an analytical expression for $R_c(\kappa)$, which is the (approximate) diffuse subsurface scattering on a curved surface with curvature κ, we employ the dipole-diffusion approximation for

$$R_d(r) = \frac{\alpha'}{4\pi}\big(R_p(z_r, r) + R_p(z_v, r)\big),$$

where

$$R_p(c, r) = \frac{c\big(1 + \sigma_{tr}\sqrt{r^2 + c^2}\big)e^{-\sigma_{tr}\sqrt{r^2 + c^2}}}{\sqrt{r^2 + c^2}^3}.$$

$z_r = 3D$ and $z_v = D(3 + 4A)$ are the offset of the real and virtual point light source in the dipole approximation;

$$\sigma_{tr} = \frac{\sqrt{3(1 - \alpha')}}{3D}$$

is the effective transport. (For an explanation of the symbols used in this sidebar, see the sections "Motivation" and "The Analytic Formulation" in the main article.) So,

$$
\begin{aligned}
R_c(\kappa) &= \int_0^\infty R_d(r)\, r\cos(\kappa r)\, dr \\
&= \frac{\alpha'}{4\pi}\left(\begin{array}{l} \int_0^\infty R_p(z_r, r)\, r\cos(\kappa r)\, dr \\ + \int_0^\infty R_p(z_v, r)\, r\cos(\kappa r)\, dr \end{array}\right).
\end{aligned}
$$
(A)

This reduces the problem to finding an analytical solution to

$$\int_0^\infty R_p(c, r)\, r\cos(\kappa r)\, dr.$$

Applying a change of variables $u = \sqrt{r^2 + c^2}$, and thus

$$du = \frac{r}{\sqrt{r^2 + c^2}}\, dr,$$

yields

$$\int_0^\infty \frac{c(1 + \sigma_{tr}u)e^{-\sigma_{tr}u}}{u^2}\cos\!\left(\kappa\sqrt{u^2 - c^2}\right)du.$$

This integral only makes sense physically over the upper hemisphere (that is, the scattering's influence does not wrap around the κ-curvature sphere horizon). Combining this observation with the exponential fall-off behavior of $R_p(c, r)$ lets us approximate $\cos\!\left(\kappa\sqrt{u^2 + c^2}\right)$ by a second-order Taylor expansion around 0, without introducing significant error to the integral:

$$
\begin{aligned}
&\int_0^\infty \frac{c(1 + \sigma_{tr}u)e^{-\sigma_{tr}u}}{u^2}\left[1 - \frac{\kappa^2(u^2 - c^2)}{2}\right]du \\
&= ce^{-\sigma_{tr}u}\left[\frac{\dfrac{-0.5c^2\kappa^2 - 1}{u}}{+\dfrac{\kappa^2}{\sigma_{tr}} + \dfrac{1}{2}\kappa^2 u}\right]_c^\infty \\
&= \left(1 - \frac{c\kappa^2}{\sigma_{tr}}\right)e^{-\sigma_{tr}c}.
\end{aligned}
$$
(B)

Combining Equations A and B yields the approximate analytical expression for $R_c(\kappa)$ in Equation 6 in the main article.

---

constant for different spherical surfaces. The estimated parameters' accuracy is very good for most cases, except very translucent materials on high-curvature spheres.

Practical Considerations

The previous derivation assumes ideal spherical-gradient illumination conditions that include negative intensities and thus are impossible to create physically. Similarly to Ma and his colleagues,[2] we instead employ shifted gradient patterns with intensities ranging from 0 to 1 ($0.5(I_X + I_1)$, $0.5(I_Y + I_1)$, and $0.5(I_Z + I_1)$), and adapt Equation 7 to compensate for this shift:

$$D \approx \frac{2}{3\kappa}\sqrt{g\,\frac{z - 1.184\dfrac{z}{ratio'}}{z + be^{-bg}}}.$$

Furthermore, the spherical-gradient lighting conditions are aligned with the global x-, y-, and z-axes, which are unlikely to align with the surface normal as required for measuring $L_{I_N}(x_o, \omega_o)$. However, we note that

$$L_{I_N}(x_o, \omega_o) = \sqrt{\begin{array}{l} L_{I_X}(x_o, \omega_o)^2 \\ + L_{I_Y}(x_o, \omega_o)^2 \\ + L_{I_Z}(x_o, \omega_o)^2 \end{array}}.$$

You can easily see this by considering the two gradients orthogonal to each other and I_N. Owing to the symmetry of $F_t(\eta, \omega_i)(\mathbf{n}(x_i) \cdot \omega_i)$ around $\mathbf{n}(x_i)$, both orthogonal gradients' responses will be zero, and only I_N yields a nonzero response. Furthermore, these spherical gradients are equivalent to first-order spherical harmonics, so we can write each gradient (for example, I_X, I_Y, and I_Z) as an affine combination of I_N and the two orthogonal gradients. The previous equality then follows

directly from light transport's linearity and the transformation's affineness.

Finally, to estimate κ, we rely on the "diffuse" normal maps obtained from the spherical-gradient observations using Ma and his colleagues' technique.[2] We compute the curvature as the angle between neighboring pixels scaled by the conversion factor for changing pixel-to-pixel distance into millimeters.

Testing Our Method

To validate our method's accuracy, we compared the scattering parameters obtained by our method with those obtained by illuminating a surface point with a narrow beam and fitting scattering parameters to the observed subsurface-scattering response. As Table 1 shows, the two sets of parameters agree.

Results

Figure 1 shows the spatially varying diffuse albedo, translucency, and absorption of a female subject acquired using an LED sphere with 156 lights. To aid in re-rendering the estimated appearance parameters, we also acquired high-resolution geometry from a stereo camera pair using Ma and his colleagues' technique.[2]

Figure 4 compares rendering results for the hybrid-normal rendering technique of Ma and his colleagues and dipole diffusion. Both approaches achieve similar qualitative results in the face's well-lit regions. However, hybrid-normal rendering, being a local shading technique, does not model soft shadow boundaries and misses the characteristic "color bleed" effect of subsurface scattering that is modeled by dipole diffusion. Both these renderings used the same four measurements under spherical-gradient illumination to obtain the model parameters.

Figure 5 shows the scattering parameters estimated from a selection of translucent materials, using an LED sphere with 346 lights. We visualized

(a)   **(b)**

Figure 4. Renderings with (a) hybrid normals and (b) dipole diffusion. The two renderings match closely in the face's well-lit areas. However, Figure 4a does not model soft shadow boundaries and misses the characteristic "color bleed" effect of Figure 4b.

the subsurface-appearance parameters by reprojecting the data onto the Stanford dragon model.

All the synthesized results in this article were rendered on the GPU in real time. If the texture and geometry were in correspondence, we used Eugene d'Eon and his colleagues' texture-space diffusion.[4] This was the case for the female subject in Figure 1, in which we captured the geometry and texture from the same vantage point. If no such natural correspondence was available, we used screen-space diffusion[5] (for example, see Figure 5).

Discussion

Our method requires a translucent sample with sufficient curvature; otherwise, the variation in the ratio in Equation 4 becomes too small to measure accurately. However, if the curvature becomes too large, then for certain ranges of D and α', a significant portion of the diffusely scattered reflectance will reside beyond the virtual sphere's

Table 1. Translucency (I_d) parameters of a single surface point for a variety of facial areas and materials. We compared the parameters obtained by our method to reference parameters obtained by fitting scattering parameters to directly observed subsurface-scattering responses.

Facial area or material	Curvature (mm⁻¹)	Linear-approximation I_d			Analytical I_d			Reference I_d		
		Red	**Green**	**Blue**	**Red**	**Green**	**Blue**	**Red**	**Green**	**Blue**
Forehead	0.108	2.42	2.01	1.79	2.30	1.97	1.79	2.26	1.97	1.75
Cheek	0.085	2.34	1.91	1.74	2.33	1.99	1.79	2.21	1.82	1.69
Lips	0.130	1.89	1.49	1.37	1.87	1.63	1.46	2.00	1.68	1.45
Red wax	0.181	2.98	1.90	1.65	2.27	1.78	1.64	2.74	1.75	1.53
Marble	0.086	7.37	5.04	3.65	6.73	5.39	4.46	7.80	5.16	4.74
Sandstone	0.101	6.62	5.17	4.02	6.95	5.38	4.18	6.04	5.38	4.28

Figure 5. Spatially varying diffusion parameters of material samples: (a) the diffuse albedo, (b) translucency, (c) absorption, and (d) an example rendering. We estimated the parameters from four observations under constant and linear spherical-gradient illumination.

Red wax · Sandstone 1 · Red marble · Sandstone 2 · Blue wax

(a)   (b)   (c)   (d)
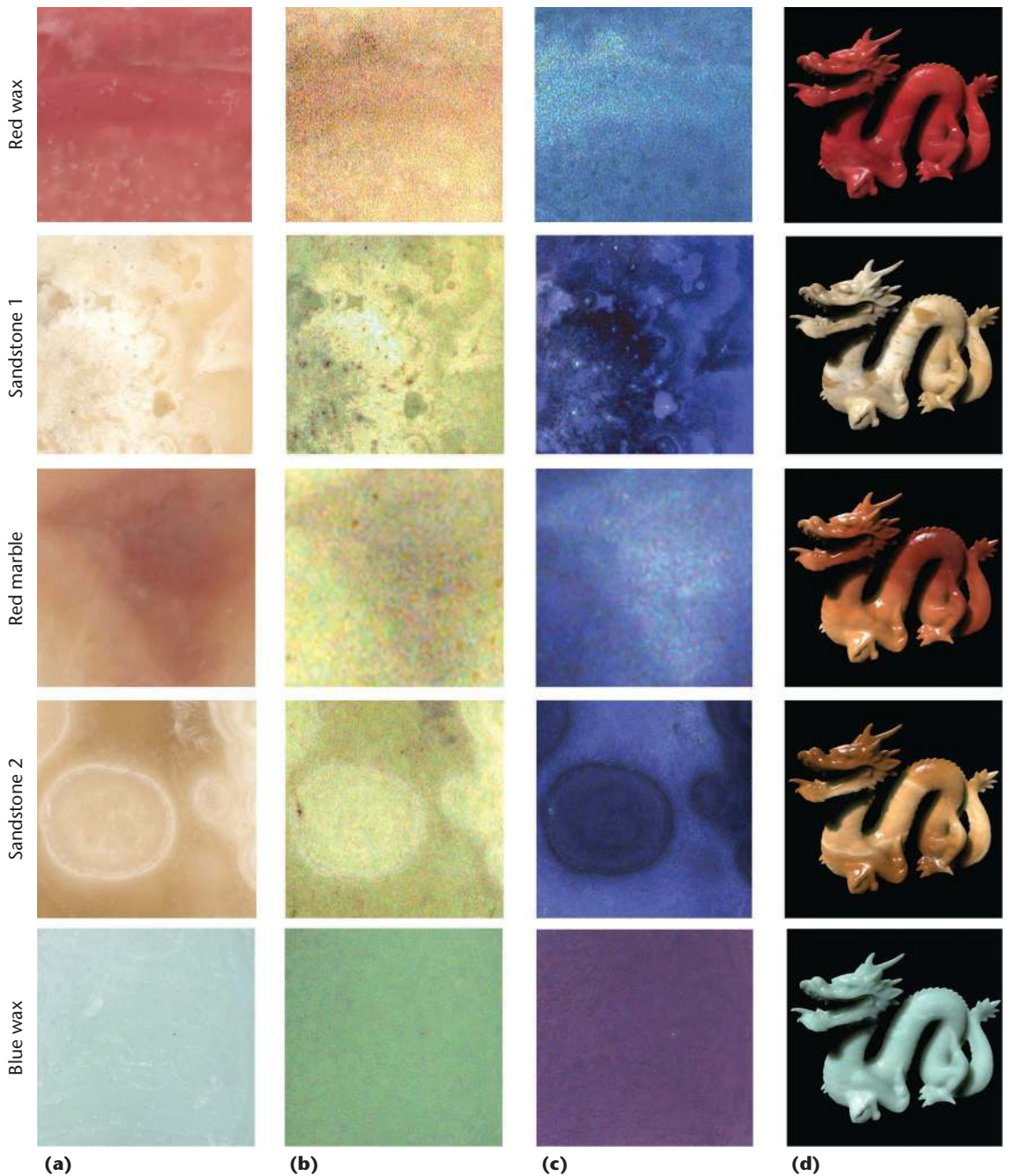
horizon. Although such a situation is mathematically valid, it makes no sense physically. Figure 3a clearly shows this for a translucency (l_d) greater than 5. (Our simulations take into account only diffuse scattering from the upper hemisphere, to better reflect physical constraints.) As a rule of thumb, we set $l_d < 0.5radius$ as a soft limit. A related source of error is the approximation of the cosine in $R_c(\kappa)$ by a second-order Taylor expansion, especially when $l_d \rightarrow 0.5radius$.

In areas with significant concavities, the measurements can also suffer from a small amount of bias due to interreflections. Also, as we mentioned before, our method assumes an index of refraction of 1.4. When the true physical index of refraction is

not 1.4, the estimates will have some errors. Generally, the larger the error on the index of refraction, the larger the error on the estimated scattering parameters. In particular, for indices of refraction larger than 1.4 and low translucency and low curvature, the numerator in Equation 7 can become negative, failing to produce a valid estimate for D.

Furthermore, surfaces cannot always locally be characterized by the mean curvature (for example, surfaces with anisotropic curvature). We compute the curvature from diffuse normals that can be biased due to interreflections and subsurface light transport. However, because we compute the mean curvature as the angle between normals, its error is generally lower than the absolute error on

the surface normals. Finally, the dipole-diffusion approximation is strictly accurate only for semi-infinite planar surfaces. Nevertheless, despite these limitations, our results show that our method can obtain accurate scattering parameters.

Possible avenues for future research include improving accuracy by using a higher-order Taylor expansion to model curvature. This will let us investigate a more general description of surface curvature that can account for anisotropic surface geometry features. Although we have applied our method to the classic dipole-diffusion model, it might be possible to extend it to newer subsurface-scattering models by employing measurements of higher-order spherical gradients.

References
1. H.W. Jensen et al., "A Practical Model for Subsurface Light Transport," *Proc. Siggraph*, ACM, 2001, pp. 511–518.
2. W.-C. Ma et al., "Rapid Acquisition of Specular and Diffuse Normal Maps from Polarized Spherical Gradient Illumination," *Proc. 18th Eurographics Conf. Rendering Techniques*, Eurographics Assoc., 2007, pp. 183–194.
3. A. Ghosh et al., "Practical Modeling and Acquisition of Layered Facial Reflectance," *ACM Trans. Graphics*, vol. 27, no. 5, 2008, article 139.
4. E. d'Eon, D. Luebke, and E. Enderton, "Efficient Rendering of Human Skin," *Proc. 18th Eurographics Conf. Rendering Techniques*, Eurographics Assoc., 2007, pp. 147–157.
5. J. Jimenez, V. Sundstedt, and D. Gutierrez, "Screen-Space Perceptual Rendering of Human Skin," *ACM Trans. Applied Perception*, vol. 6, no. 4, 2009, article 23.

Yufeng Zhu *is a PhD student in the University of British Columbia's Computer Science Department. His research interests are physically based animation, computational mathematics, and optimization. He previously was a graduate research assistant at the University of Southern California Institute for Creative Technologies. Zhu received a master's in computer science from USC. Contact him at mike323zyf@gmail.com.*

Pradeep Garigipati *is a master's student in Texas A&M University's Computer Science Department. His research interests are computer graphics and parallel computing. He previously was a graduate research intern in the Graphics Lab at the University of Southern California Institute for Creative Technologies. Garigipati received a B.Tech. in computer science and engineering from the National Institute of Technology, Durgapur. He is a student member of ACM. Contact him at pradeep.garigipati@gmail.com.*

Pieter Peers *is an assistant professor in the College of William & Mary's Computer Science Department. His research interest is data-driven appearance modeling. He previously was a senior researcher at the Graphics Laboratory at the University of Southern California Institute for Creative Technologies and a research assistant professor at USC's Viterbi School of Engineering. Peers received a PhD in computer science from KU Leuven. Contact him at ppeers@siggraph.org.*

Paul Debevec *is the associate director of graphics research at the University of Southern California Institute for Creative Technologies and a research professor of computer science at USC. His research has focused on image-based modeling and rendering, with specializations in architecture, high-dynamic-range lighting, and human facial capture. He is the vice president of Siggraph and has received an Academy Award for his work on the Light Stage facial-capture systems. Contact him at debevec@ict.usc.edu.*

Abhijeet Ghosh *is a lecturer in Imperial College London's Department of Computing. His main research interests are appearance modeling, realistic rendering, and computational photography. Previously, he was a senior researcher and research assistant professor at the University of Southern California Institute for Creative Technologies. Abhijeet received his PhD in computer science from the University of British Columbia. His doctoral dissertation, "Realistic Materials and Illumination Environments," received an Alain Fournier Award. He holds a Royal Society Wolfson Research Merit Award at Imperial College London. Contact him at abhijeet.ghosh@imperial.ac.uk.*

Selected CS articles and columns are also available for free at http://ComputingNow.computer.org.